Chapter 5 Regional-Scale Simulation of Ground-Water Age and CFC-11 Transport at the Mirror Lake Site, New Hampshire

5.1 Introduction

Investigators of the USGS, and others, are trying to characterize large-scale flow and transport properties of the ground-water flow system beneath the Mirror Lake drainage basin, located in north-central New Hampshire (fig. 5-1). Background hydrogeologic information and summaries of previous investigations are provided by Winter (1984; 1985), Winter and others (1989), Shapiro and Hsieh (1991), and Hsieh and others (1993). A wide range of investigative methods are being applied, including the use of large-scale model calibration. A large-scale flow model was calibrated by Tiedeman and others (1997) using measured hydraulic head and streamflow to estimate hydraulic conductivity of the glacial drift and fractured rock. Continuing efforts include calibration of transport models of advective travel time (C.R. Tiedeman, personal commun., 1996) and tritium and CFC-12 transport with matrix diffusion (Shapiro, 1996; Shapiro and others, 1996). Harte (1992) and Harte and Winter (1995) modeled cross-sectional flow between the glacial drift and bedrock, and examined the role of heterogeneity in the glacial drift in controlling local vertical flow. Chapter Four of this thesis addresses degradation of CFC's at the top of the saturated zone that complicates interpretation of saturated-zone concentrations through transport modeling. One method of interpreting environmental tracer information is to convert measured concentrations to ground-water ages. The observed distribution of ages can be compared to a transport model of ground-water age, as developed in Chapter Two.

In this chapter, a numerical transport model is used to simulate ground-water age and CFC-11 concentrations in the Mirror Lake basin. These alternative approaches to

simulating tracer information are compared and contrasted. The effective porosity of bedrock is varied from 0.05 to 0.005. The impact of matrix diffusion and stream-aquifer interaction on CFC-11 concentrations is illustrated.

5.2 Background

5.2.1 Regional-Scale Flow Modeling at Mirror Lake site

Tiedeman and others (1997) calibrated a regional-scale three-dimensional ground-water flow model to measured water levels and streamflow in the Mirror Lake watershed. Calibration of the flow model used a non-linear optimization procedure coupled with the ground-water flow model (Hill, 1992). In addition to providing an estimate of regional-scale hydraulic properties, hydraulic conductivity and recharge, this model was used to characterize the ground-water flow beneath the Mirror Lake watershed. Figure 5-1 shows their finite-difference grid and important hydrologic features of the modeled area. A subset of this model domain, indicated in the figure, is re-gridded for the transport simulations here.

Ground-water pathline analysis was used to identify the ground-water drainage basin of Mirror Lake and streams that flow into Mirror Lake (Tiedeman et al., 1997). Figure 5-2 is a schematic of the three-dimensional ground-water drainage basin for Mirror Lake. The area of the land surface from which infiltration eventually reaches Mirror Lake is considerably larger than the surface-water drainage basin delineated from topography. Furthermore, the subsurface extent of the volume of aquifer containing water that is flowing towards Mirror Lake and its tributaries extends outside the land surface boundaries of the ground-water basin. Some of the infiltration at high elevations flows downward and beneath the adjacent ground-water basin of Norris Brook, before eventually turning towards Mirror Lake and lower elevations of the stream network.

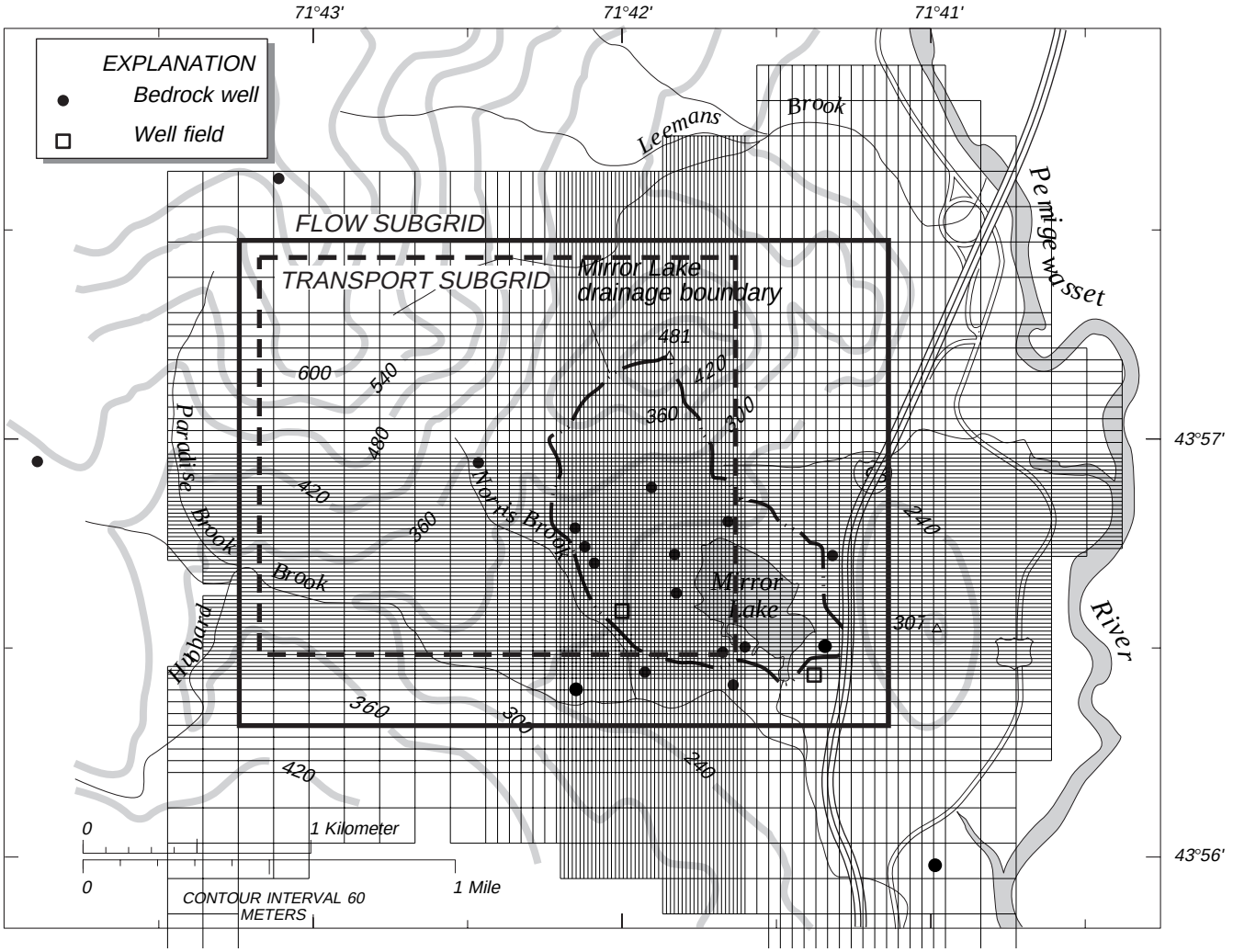

Figure 5-1 Location map of Mirror Lake site, New Hampshire, regional-scale finite-difference grid (Tiedeman et al., 1997), and flow and transport subgrids.

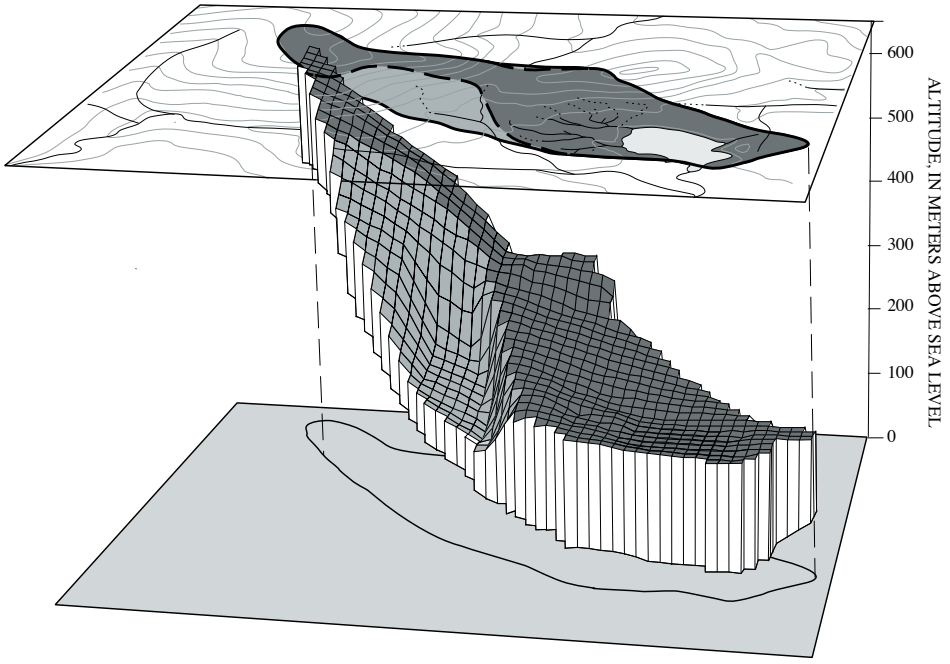

Figure 5-2. Mirror Lake ground-water drainage basin (Tiedeman et al., 1997).

5.2.2 Environmental Tracers and Ground-Water Age at the Mirror Lake Site

Age dating of ground water at the Mirror Lake site has met with limited success. The tritium-helium age-dating method cannot be used in bedrock ground waters because of a local source of helium (Drenkard et al., 1993). Busenberg and Plummer (1996) present results of CFC and tritium sampling. Spatial patterns of CFC-derived ground-water ages cannot be easily related to recharge/discharge in the ground-water basin (see fig. 4-3). The general temporal pattern of CFC-12 dates and tritium concentrations is similar to the tritium input function from the atmosphere (fig. 5-3). Recent recharge has tritium concentrations in the range of 10-20 TU, while water older than about 50 years has very little tritium due to decay. However, the peak tritium concentrations occurred in the atmosphere in 1963 in New Hampshire, while the peak from tritium and CFC-12 data appears to occur several years later. More significantly, the peak tritium concentrations

are well below the 250-300 TU range that would be expected for early-1960's recharge, accounting for decay to 1992 (Busenberg and Plummer, 1996).

Shapiro (1996) suggests that the temporal pattern of tritium and CFC-derived recharge dates may be caused by large-scale matrix diffusion. Matrix diffusion affects tritium and CFC concentrations differently because of differences in diffusion coefficients, but more importantly, because their source input functions are very different (Plummer et al., 1993). The effect of matrix diffusion is, in part, to reduce the sharp peak of the tritium input function. Diffusion has less impact on the concentrations of CFC's, because CFC atmospheric concentrations have increased gradually in time. Shapiro's (1996) approach was to treat all ground-water samples as if they are drawn from a one-dimensional flow system, but the sample location along the flowpath is unknown. By adjusting diffusion coefficients in the bedrock and glacial drift, the general pattern of tritium and CFC-12 concentrations was matched.

C.R. Tiedeman (personal commun., 1994) modeled advective travel time using the large-scale flow model of Tiedeman and others (1997). A match could be obtained between the range in advective travel time to a bedrock well, and the ground-water ages determined from CFC-12. However, the calibrated effective porosity was considered too high to be representative of the bedrock at the Mirror Lake site.

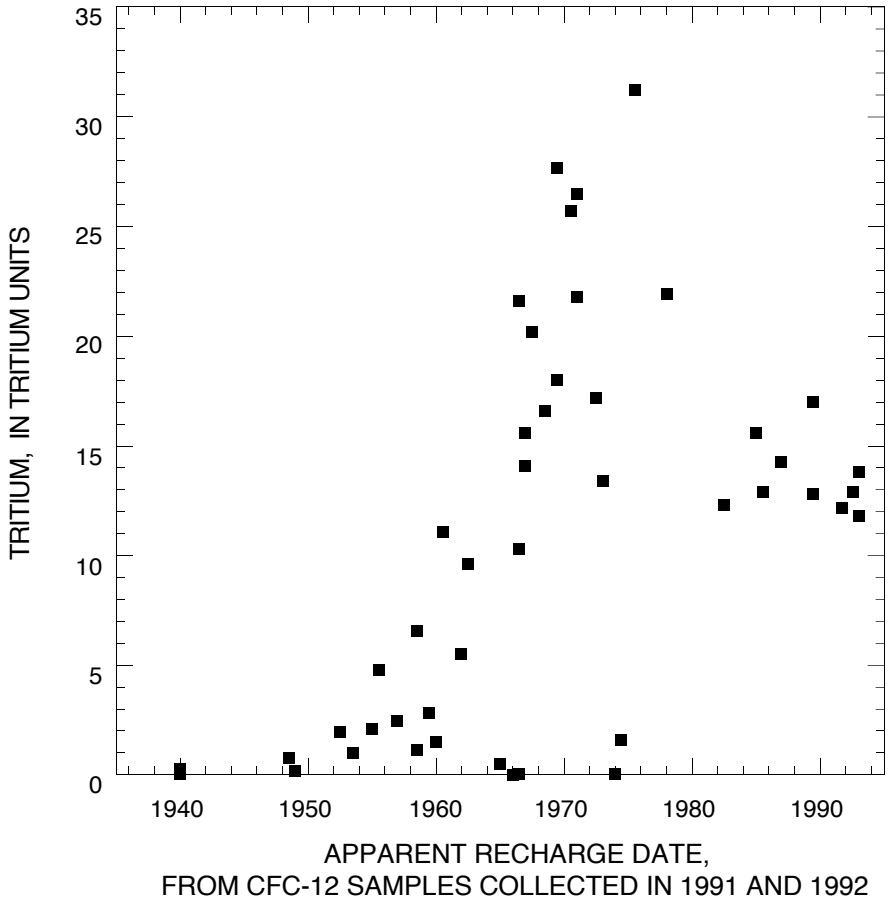

Figure 5-3 Tritium concentrations versus apparent recharge dates from CFC-12 concentrations in ground-water samples from drift piezometers and bedrock wells at Mirror Lake site (Busenberg and Plummer, 1996).

5.2.3 Scope of this study

The goal of this investigation is to illustrate the application of the methods developed in Chapter Two to simulation of ground-water age at the Mirror Lake site. The impact of matrix diffusion on ground-water age is investigated directly by including this process in the age transport model. The results of ground-water age simulation are compared to simulations of CFC-11 transport with and without matrix diffusion.

5.3 Model Construction

The flow and transport model used here is derived from that of Tiedeman and others (1997) in two main steps. The original nonlinear model is converted to a linear flow model by computing horizontal transmissivities from the calibrated model heads. The model structure and calibration results used here correspond to Parameterization D of Tiedeman and others (1997). Secondly, the model is re-gridded by subdividing larger model cells into square cells having the same dimensions as the smallest cells in the full model. Uniform horizontal gridding is required for the transport model modified and used here (Konikow et al., 1996).

First, the calibrated full model heads are used to compute saturated thicknesses of each model cell. The transmissivity of each model cell is then computed as the product of the saturated thickness and the calibrated hydraulic conductivity. Cells in which the hydraulic head is below the bottom of the cell are removed from the model domain (fig. 5-4). Recharge is applied to the top active cell at each location.

Ground water flows into streams in the model depending on the difference between the hydraulic head and a prescribed stream hydraulic head, estimated from topography. The streambed conductance is large, hence where streamflow is active, the difference between the head in the aquifer and in the stream is small. Because the transport model used here (Konikow and others, 1996) is not compatible with the stream simulation package used by Tiedeman and others (1997), the flux in each stream cell is computed for the calibrated model and used as a prescribed well flux (fig. 5-4). This procedure yields computed hydraulic heads and fluxes in the model that are essentially identical to the nonlinear model version, but only for this particular parameterization. If any of the hydraulic properties were changed, such as hydraulic conductivity, recharge or stream head, then the original nonlinear model with stream cells would have to be rerun and the conversion process described here repeated.

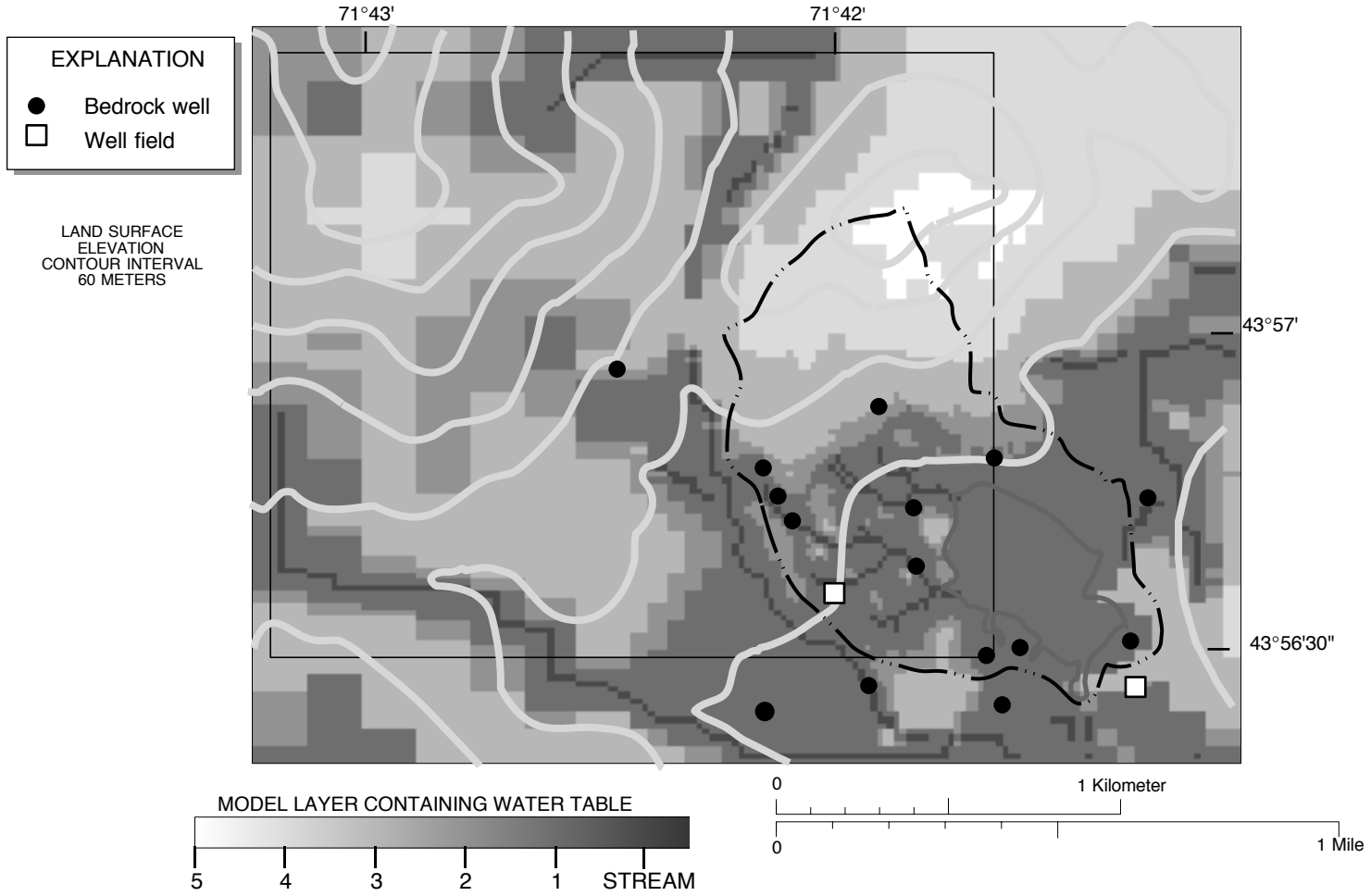

Figure 5-4. Stream cells and shading of uppermost active model layer containing water table in flow subgrid using model structure and calibrated parameters of Tiedeman and others (1997).

A uniform discretization subgrid is constructed for application of the transport model of Konikow and others (1996). The subgrid uses the smallest model cell size shown in figure 5-1 for all cells; the horizontal discretization is 16.67 by 16.67 m. Within the finest gridded portion of the full model there is a one-to-one correspondence between cells of the full grid and cells of the subgrid. Outside this area, larger cells are divided in thirds or ninths in each direction, depending on the cell size. A nearest neighbor procedure is used to assign the subgrid cells parameters from the full grid parameters.

Only a portion of the flow subgrid is used for solute transport simulations. One reason for choosing this transport subgrid is that an area of very high transport velocities in the sand and gravel unit south of Mirror Lake can be excluded. Inclusion of this area in a transport model imposes severe time-step restrictions. The primary goal of these simulations is to characterize the transport conditions in the glacial drift and bedrock in the Mirror Lake watershed to the northwest of the lake, and the sand and gravel unit to the south of Mirror Lake has essentially no effect on transport through the higher portions of the flow system.

The model structure used here is that of Tiedeman and others (1997). The thickness of the glacial drift is assumed to be 9 m, except in the vicinity of Mirror Lake where the thickness varies from 0 m to over 40 m based on drilling and seismic survey data (Winter, 1984; Tiedeman et al., 1997). The glacial drift is divided vertically into two model layers of equal thickness. The bedrock is divided vertically into three model layers having thicknesses of 30, 60, and 60 m, from top to bottom, respectively.

Tiedeman and others (1997) prescribed no-flow boundaries on all sides and on the bottom of the model domain. Here, computed heads in the model of Tiedeman and others (1997) at the flow subgrid boundary are used as prescribed heads for the smaller region. Uniform recharge is applied on the top of the saturated zone, except on Mirror

Lake itself. Mirror Lake is modeled as a zone of prescribed hydraulic head in the top saturated model layer.

In addition to geometric properties, some of the parameters of the model were not calibrated by Tiedeman and others (1997) because the model parameters were not sufficiently sensitive to the observed head and streamflow measurements. The hydraulic conductivity of a region of sand and gravel south of Mirror Lake is assumed to have a hydraulic conductivity of 5×10^{-5} m/s (T.C. Winter, personal commun., 1994). The lacustrine lake sediments underlying much of Mirror Lake are prescribed a hydraulic conductivity of 1×10^{-9} m/s (Rosenberry and Winter, 1993).

Estimated parameters of the flow model of Tiedeman and others (1997) for their Parameterization D include recharge, 280 mm/yr, glacial drift hydraulic conductivity, 1.74×10^{-6} m/s, bedrock hydraulic conductivity in the lower part of the basin, 3.21×10^{-7} m/s, and bedrock hydraulic conductivity in the upper part of the basin, 6.26×10^{-8} m/s.

5.3.1 Flow model results

The flow model results are essentially as described by Tiedeman and others (1997). The water table (fig. 5-5) occurs in the glacial drift model layers in the lower elevations of the watershed, and near flowing streams. At higher elevations, the water table is simulated in bedrock, and in a small part of the basin the water table is more than 90 m below the top of the bedrock surface. The water-table gradients are steepest in higher elevations of the watershed where the glacial drift is unsaturated and the bedrock has lower hydraulic conductivity than at lower elevations.

The simulated hydraulic head in the deepest model layer (fig. 5-6) is somewhat smoother than the water table configuration. Ground water generally flows from the northwest to the southeast, as indicated by the three-dimensional ground-water basin (fig. 5-2). Discharge to larger streams is evident in hydraulic head contours, even at depth in the bedrock.

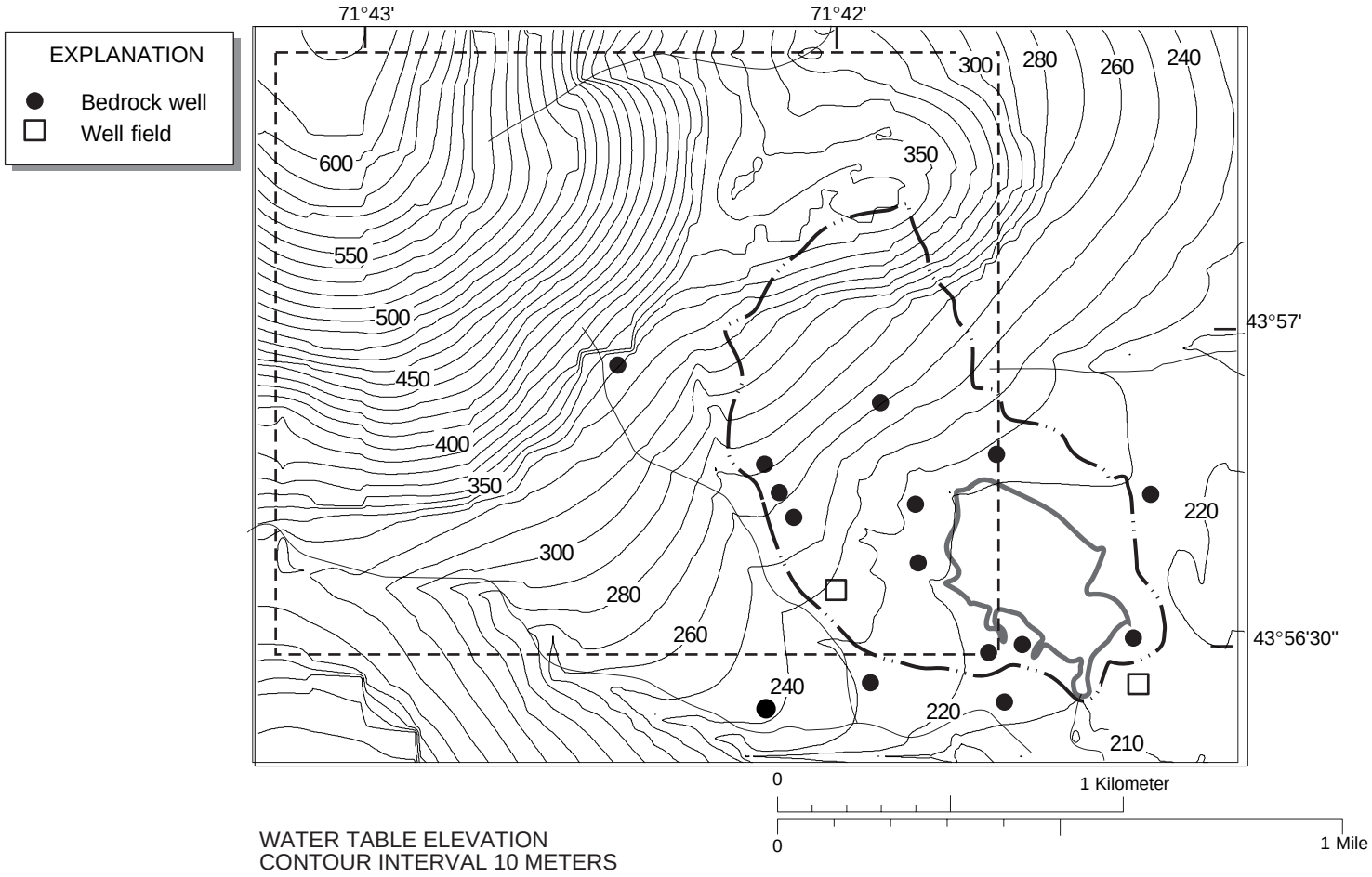

Figure 5-5 Simulated water-table elevation in flow subgrid using model structure and calibrated parameters of Tiedeman and others (1997).

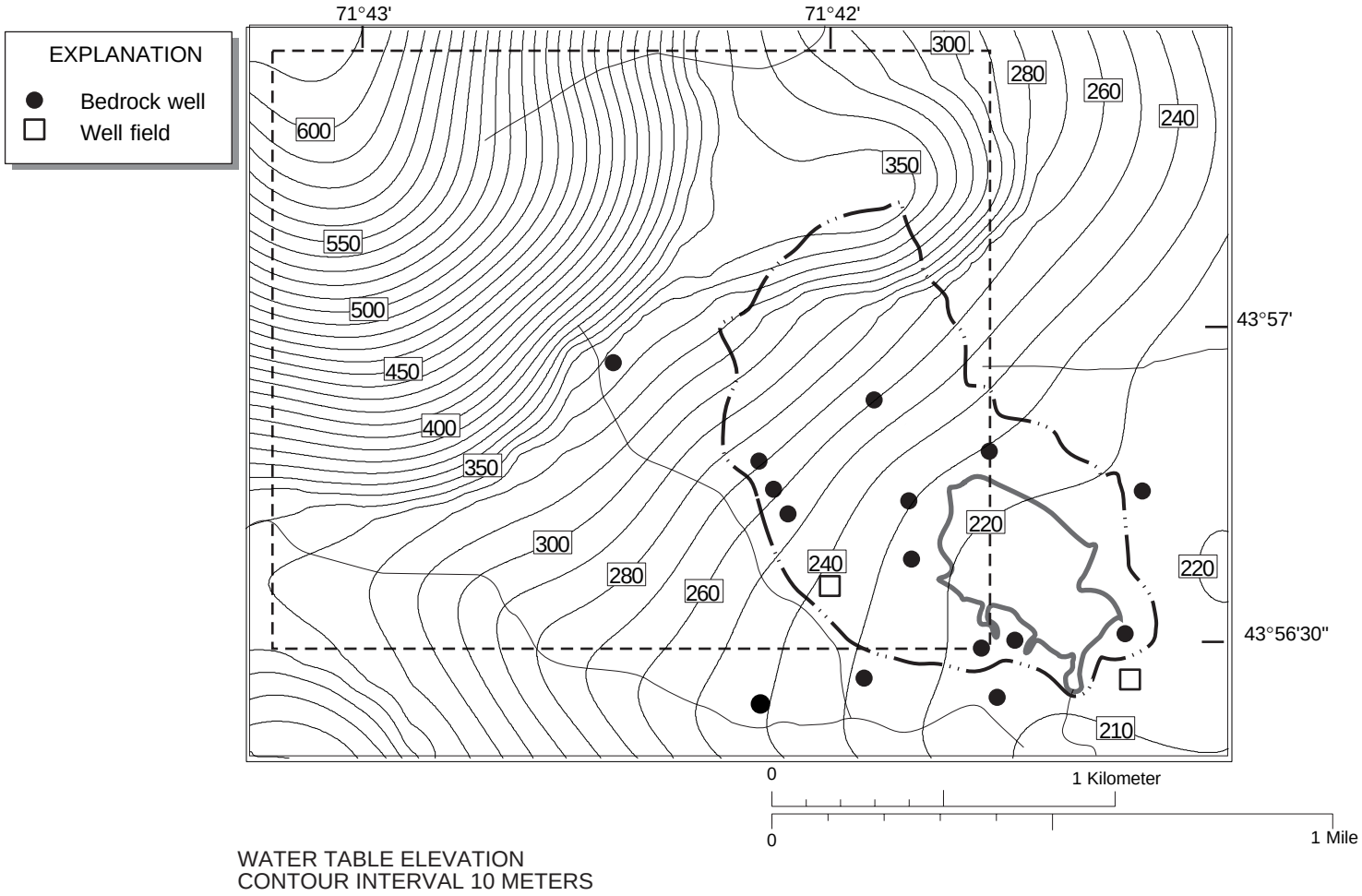

Figure 5-6 Hydraulic head in bottom model layer (5) representing bedrock between 90 and 150 m below bedrock surface.

5.4 Ground-Water Age

Ground-water age is simulated using the transport model developed in Chapter Two. Boundary conditions for the age simulation are incoming age of zero in recharge and in streamflow entering the aquifer. Only advective transport is considered in these simulations. The porosity of the glacial drift is assumed to be 0.2 for all simulations. Simulations are conducted for bedrock effective porosities of 0.05 and 0.005. For comparison, the low porosity value is representative of transport in the fractures alone, while the higher porosity value is assumed to represent the steady-state age as affected by matrix diffusion, where the rock matrix is assumed to have porosity of 0.045. Both of these values, 0.005 for effective porosity in fractures, and 0.05 for total porosity, may be too high for the fractured crystalline rock at the Mirror Lake site (Hsieh et al., 1993, Wood et al., 1996), but are used here for illustrative purposes.

Recharge water entering the saturated zone at the water table has an age of zero, by definition. In lower parts of the watershed, the water table occurs in the glacial drift, hence water must flow vertically downward before entering the bedrock. This leads to older ages in the upper bedrock in the lower parts of the watershed (fig. 5-7). At higher elevations, the glacial drift is unsaturated, and the water table, where recharge occurs, is in the bedrock. Hence, the age of water in the upper part of the bedrock in these areas is low (fig. 5-7). The oldest ages in the upper bedrock occur at discharge areas in the lower parts of the basin. Old water also occur in the upper bedrock beneath ground-water divides, where the head gradients and velocities are low.

The factors affecting age in the deep bedrock are similar to those for the upper bedrock, but ages are generally older (fig. 5-8) because of the additional time required to move down through 90 meters of bedrock. Youngest ages occur at higher elevation where the upper bedrock is unsaturated. Ages greater than 50 years occur in much of the area near Mirror Lake.

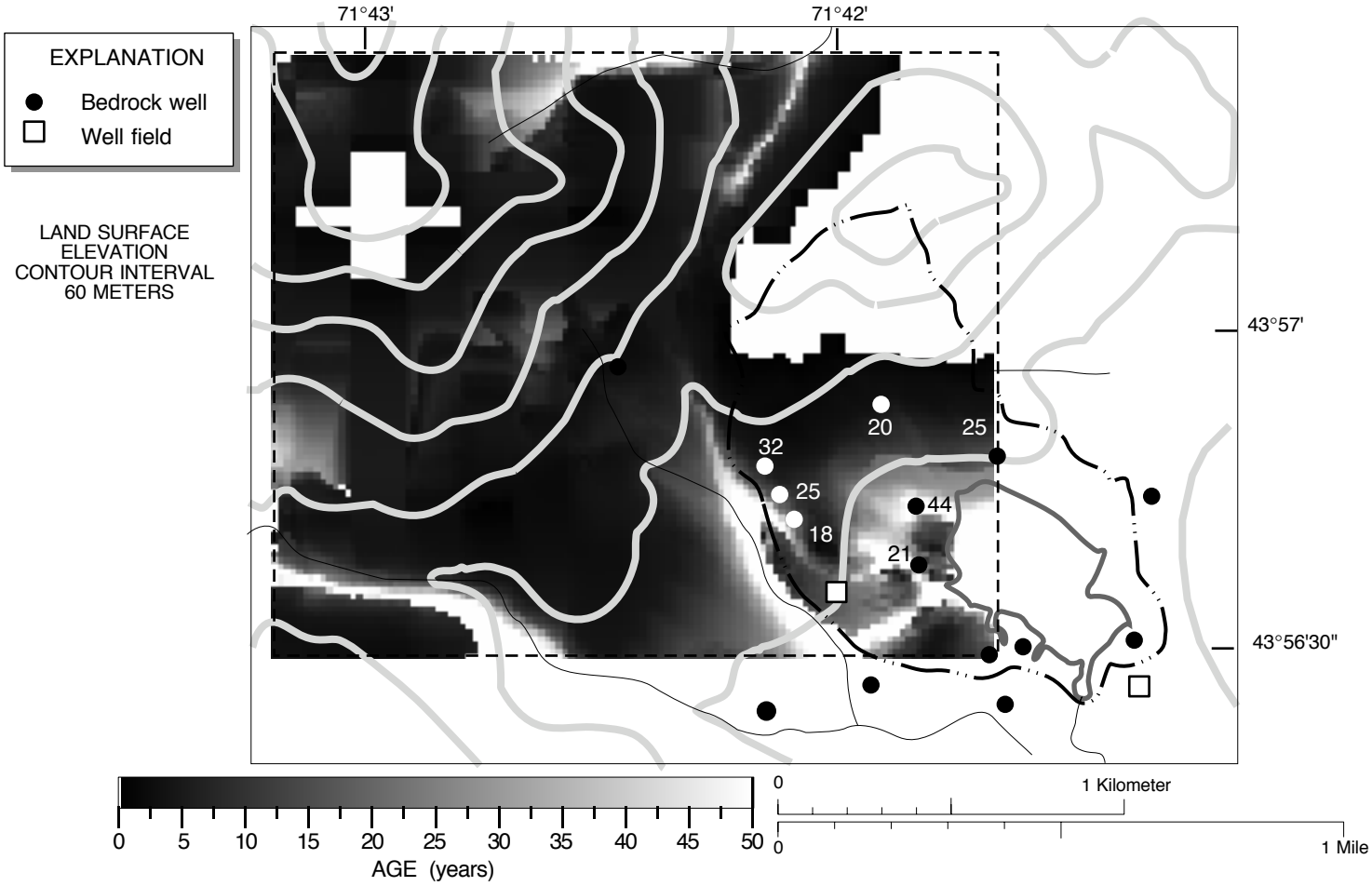

Figure 5-7 Simulated ground-water age in upper bedrock from bedrock surface to 30 meters below bedrock surface for advection only using bedrock effective porosity of 0.05. Numbers are apparent ages in shallowest sampled fracture zone from CFC-12 (Busenberg and Plummer, 1996).

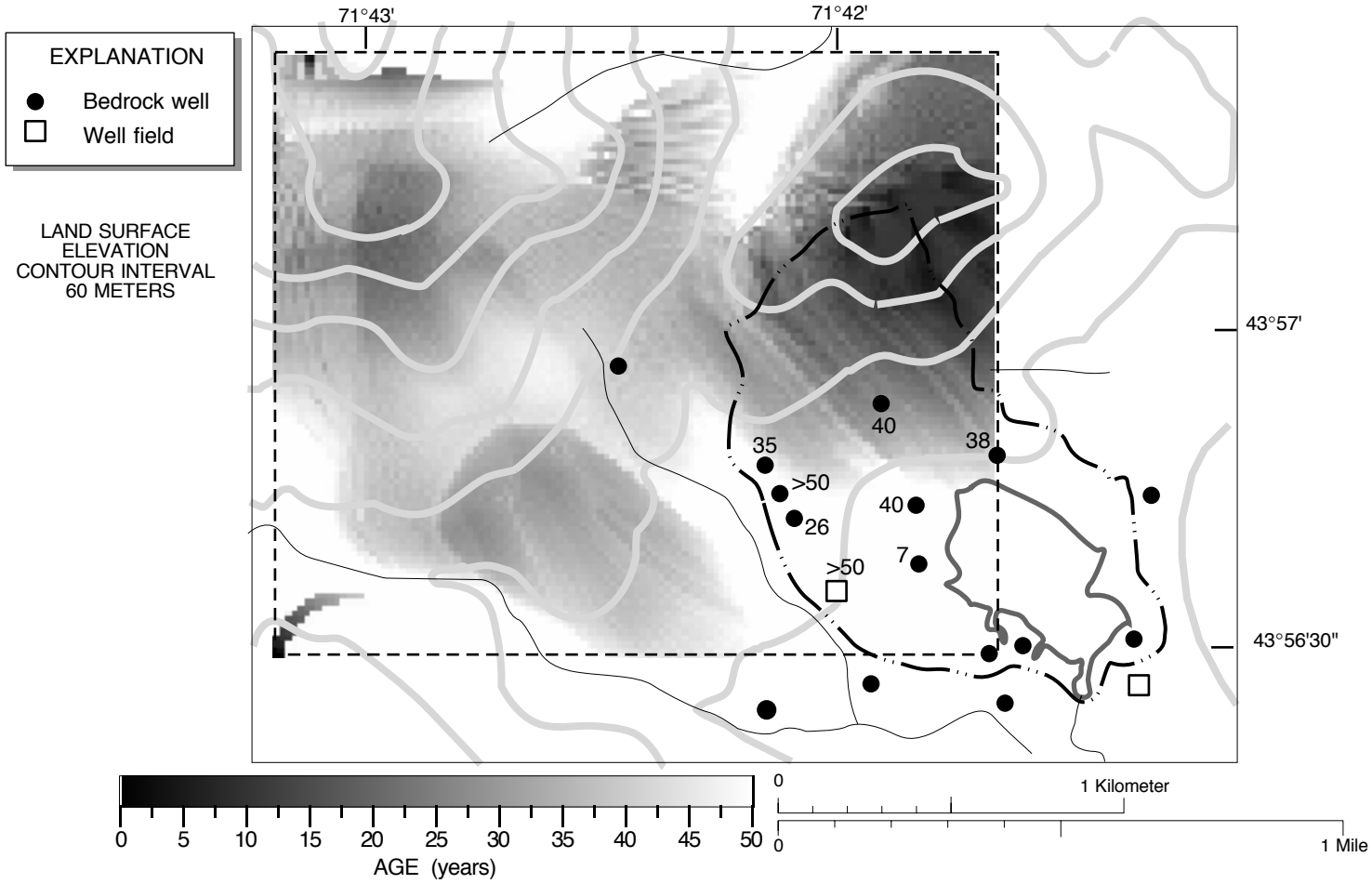

Figure 5-8 Simulated ground-water age in deep bedrock from 90 meters below bedrock surface to 150 meters below bedrock surface for advection only using bedrock effective porosity 0.05. Numbers are apparent ages in deepest sampled fracture zone from CFC-12 (Busenberg and Plummer, 1996).

With a factor of ten reduction in bedrock porosity to 0.005, ages are generally younger in bedrock layers, as expected. The spatial pattern of ages in the upper bedrock (fig. 5-9) is similar to the higher porosity case. Ages are generally less than a couple of years throughout the upper bedrock, and do not exceed 30 years in any locations. Similarly, ages are younger in the deep bedrock (fig. 5-10), although the spatial pattern is similar to the high porosity case.

Ideally, apparent ages from CFC-12 concentrations (Busenberg and Plummer, 1996) could be used to calibrate the flow and transport model. This model has not been calibrated, but preliminary comparisons can be made between observed apparent ages and simulated ages. The apparent ages are generally higher than the simulated ages for the low porosity case, even though this porosity is probably too high to represent the effective porosity for transport in the fractures. These results are consistent with travel time calibrations (C.R. Tiedeman, personal commun., 1994). The high porosity value, which may represent steady-state age as affected by matrix diffusion, yields ages more similar to the apparent ages. However, the porosity of 0.05 is higher than the measured 0.01 to 0.02 values on rock cores (Wood et al., 1996).

For the deep bedrock, several of the old waters are located in the portion of the basin where simulated ages for the high porosity case exceed 40 years. However, other nearby wells exhibit much younger ages. The young age observed in well T1 (7 years on the figs. 5-8 and 5-10) is in an area where the simulated ages in the upper bedrock are quite variable. T1 is located near Mirror Lake, but on a topographic high. This configuration leads to spatially variable ages; young water in the bedrock under the topographic high where the saturated glacial drift is thin, and old water in the lower parts where deep groundwater is discharging upward. Given the heterogeneous nature of the fracture flow system, these complex flow patterns would be expected to lead to highly variable ages in fractures intersecting bedrock wells.

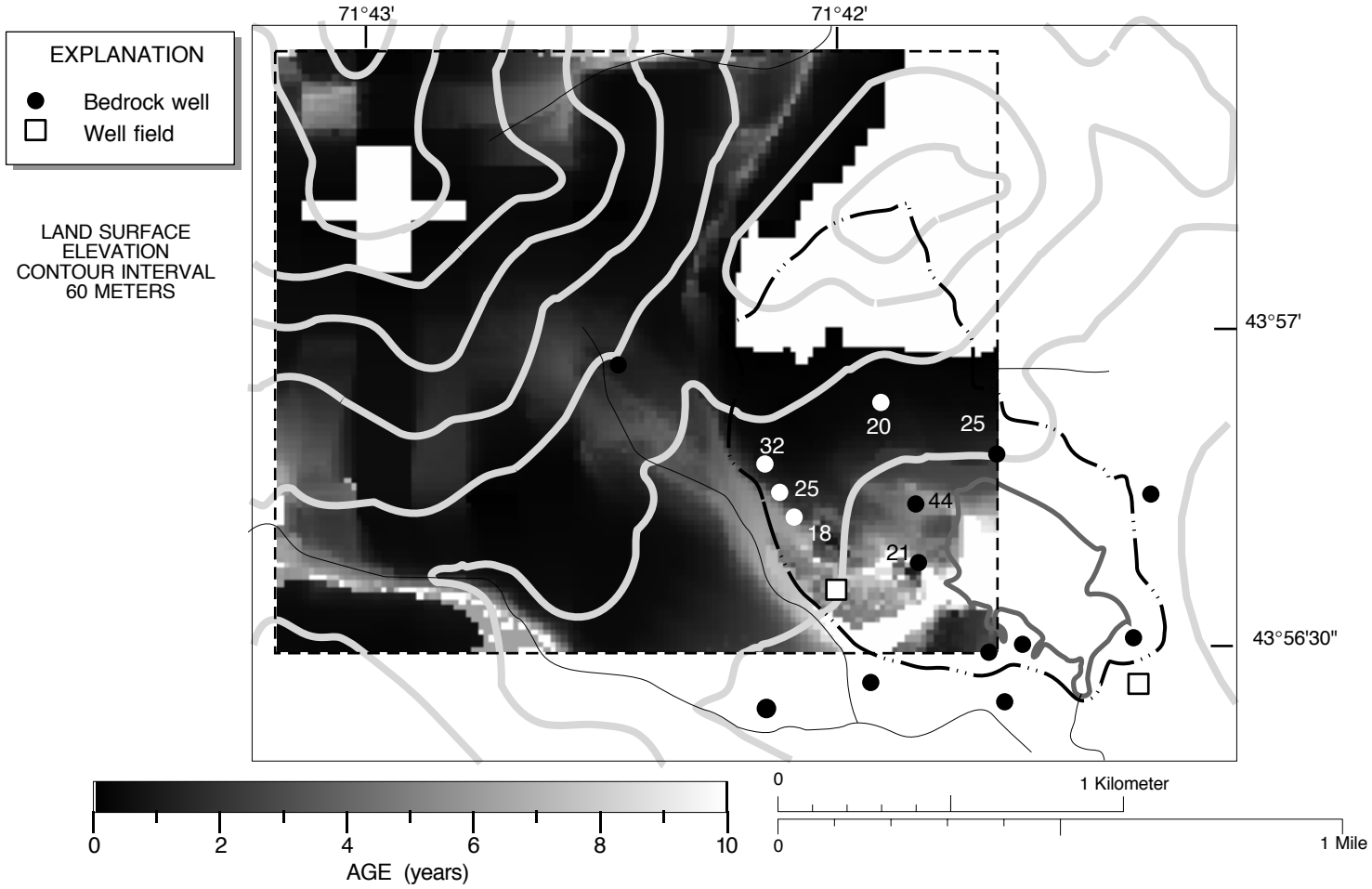

Figure 5-9 Simulated ground-water age in upper bedrock from bedrock surface to 30 meters below bedrock surface for advection only using bedrock effective porosity of 0.005. Numbers are apparent ages in shallowest sampled fracture zone from CFC-12 (Busenberg and Plummer, 1996). The age grayscale ranges from 0 to 10 years.

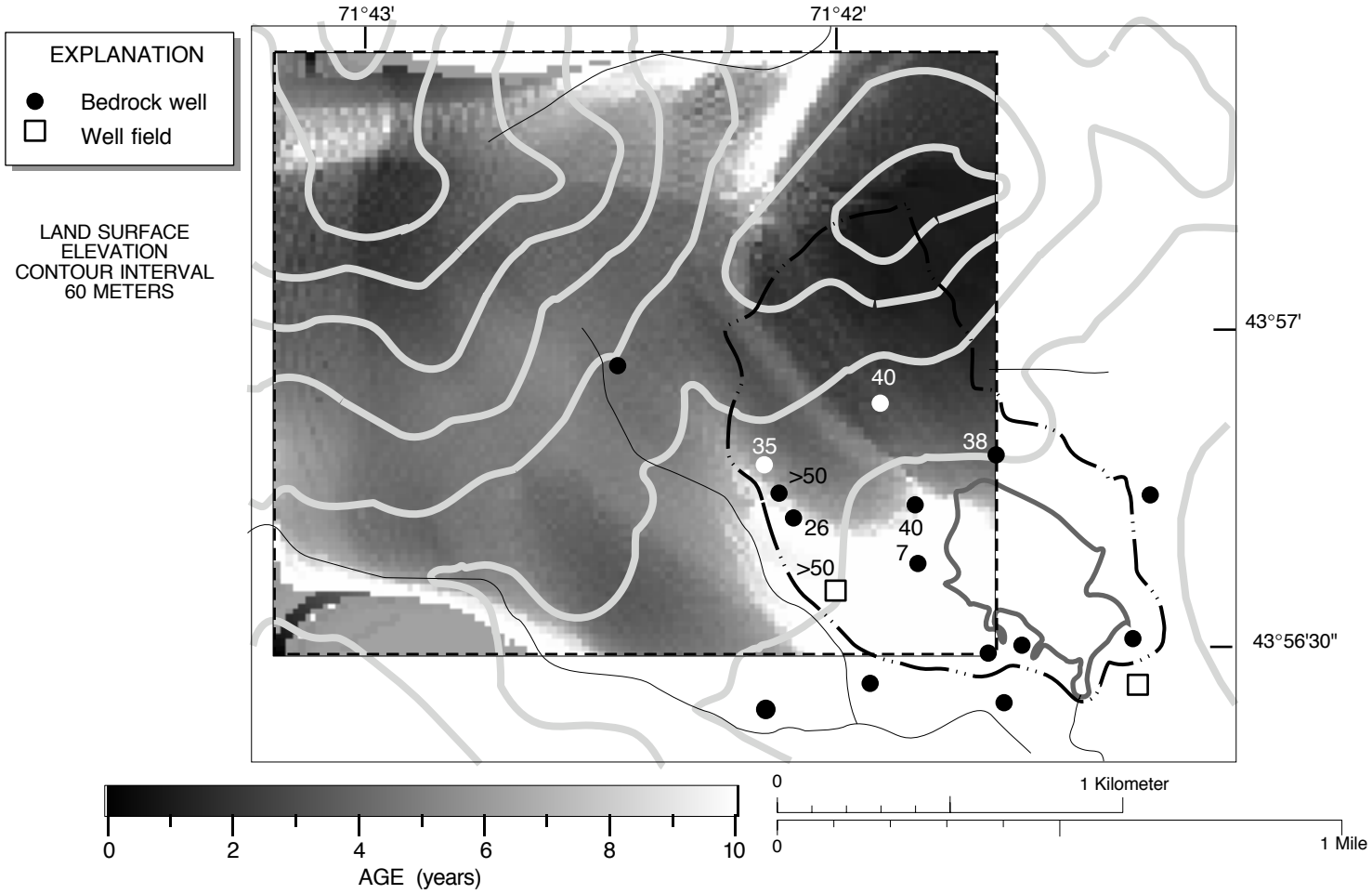

Figure 5-10 Simulated ground-water age in deep bedrock from 90 meters below bedrock surface to 150 meters below bedrock surface for advection only using bedrock effective porosity of 0.005. Numbers are apparent ages in deepest sampled fracture zone from CFC-12 (Busenberg and Plummer, 1996). The age grayscale ranges from 0 to 10 years.

5.5 CFC-11 Transport

Fifty years of CFC-11 transport is simulated to compare with the age transport results. The CFC-11 input function in recharge is based on global atmospheric levels and an assumed recharge temperature of about 6 °C. Based on observed CFC-11 degradation near an area of streamflow loss to the aquifer (Chapter Four), the CFC-11 concentration in streamflow to the aquifer is assumed to be zero.

5.5.1 Advective Transport

For advective transport alone, the CFC-11 concentration generally corresponds directly to the age, although the correspondence is not exactly linear. The atmospheric levels of CFC-11 (fig. 4-1) have been increasing almost linearly since the early 1960's, but before 1960 concentrations were increasing at a much slower rate. Thus, a linear relation is represented between CFC-11 and ages for waters younger than about 35 years, whereas very low, but nonzero, concentrations occur in older waters up to about 45 years old.

High CFC-11 concentrations are simulated in the upper bedrock (fig. 5-11) in parts of the basin where the glacial drift is unsaturated. As with the simulated ages, the CFC-11 concentrations in the upper bedrock are spatially variable in the area near a topographic high adjacent to Mirror Lake. The zero-CFC water discharging from stream to the glacial drift does not have a widespread impact on concentrations in the bedrock. If this impact were significant, areas of low CFC-11 concentrations would be observed in areas with very young ages.

The deep bedrock also exhibits high CFC-11 concentrations (fig. 5-12) beneath the topographic high where the water table is simulated deep in the system. However, CFC-11 concentrations are low in most of the deep bedrock for the high-porosity case.

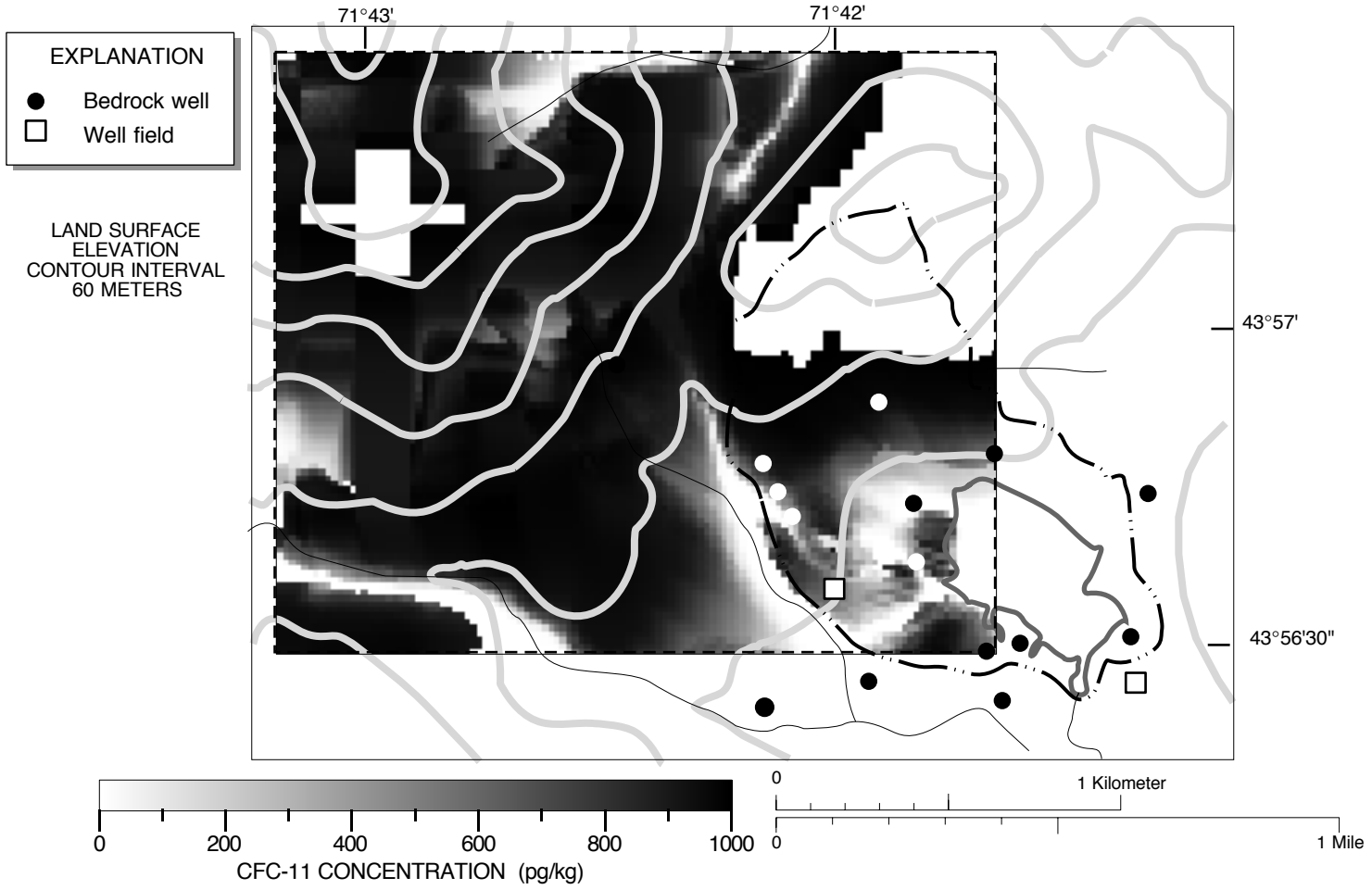

Figure 5-11 Simulated CFC-11 concentrations in upper bedrock from bedrock surface to 30 meters below bedrock surface for advection only using bedrock effective porosity of 0.05.

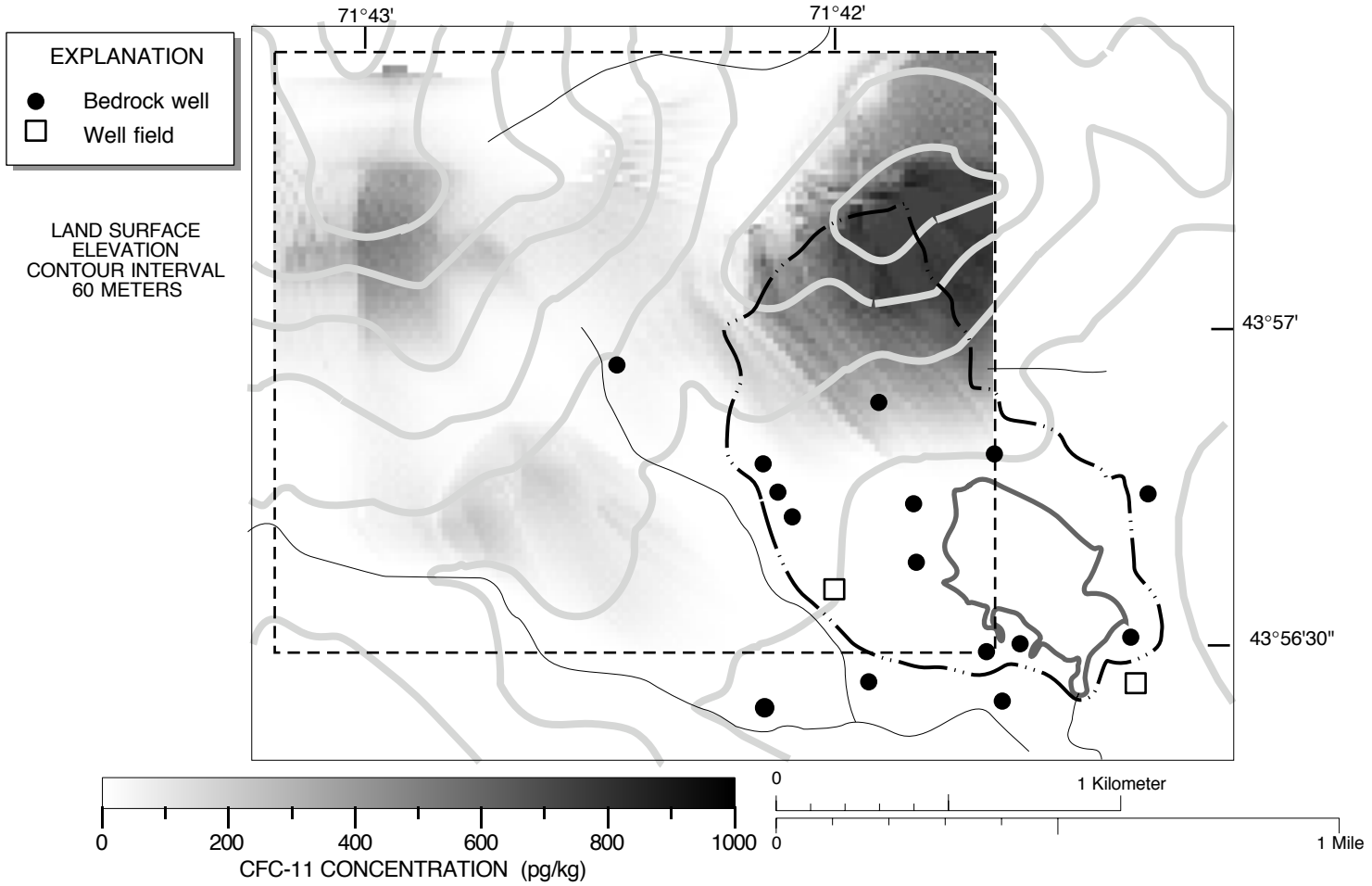

Figure 5-12 Simulated CFC-11 concentrations in deep bedrock from 90 meters below bedrock surface to 150 meters below bedrock surface for advection only using bedrock effective porosity of 0.05.

CFC-11 concentrations are higher in bedrock for the lower porosity simulation, under advection alone. These results are similar to those for the age simulations: the ground-water ages are younger in the bedrock using bedrock effective porosity of 0.005. Lowest concentrations occurring in the Mirror Lake basin are less than 25 pg/kg beneath the western shore of the lake where ground water is discharging upward through the low-permeability lake-bed sediments.

One difference between the age and CFC-11 simulations is in an area of streamflow loss to ground water. This occurs just to the southeast (down and to the right in the figure) of the lowest of the three wells along the western boundary of the Mirror Lake drainage basin. The upper bedrock concentrations here reflect, in part, stream loss which is assumed to have zero CFC-11 because of degradation in the stream bottom. This water has young age, but also has low CFC-11 concentrations, opposite the general relation where degradation is not present. However, this streamloss water apparently does not flow downward to the deep bedrock; there concentrations are higher reflecting rapid velocity of recent recharge through the system. This pattern is also shown in the higher porosity case (fig. 5-11), but is not as distinct because the upper bedrock has low CFC-11 concentrations in several locations in that case. This occurrence of streamloss water in the upper bedrock would lead to apparent ages of old water in the upper bedrock and young water in the deep bedrock, which is observed in some bedrock wells at Mirror Lake (fig. 4-3).

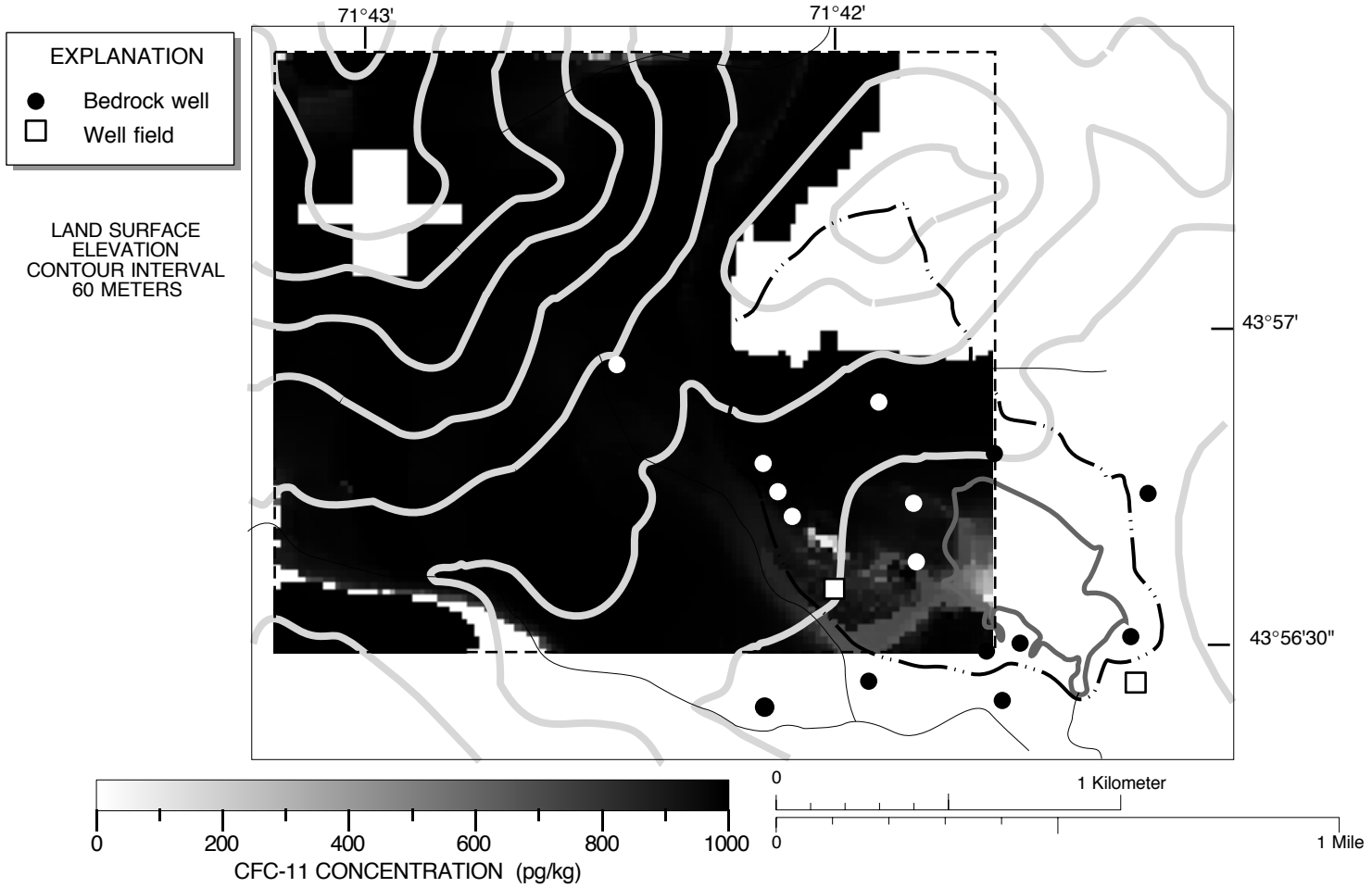

Figure 5-13 Simulated CFC-11 concentrations in upper bedrock from bedrock surface to 30 meters below bedrock surface for advection only using bedrock effective porosity of 0.005.

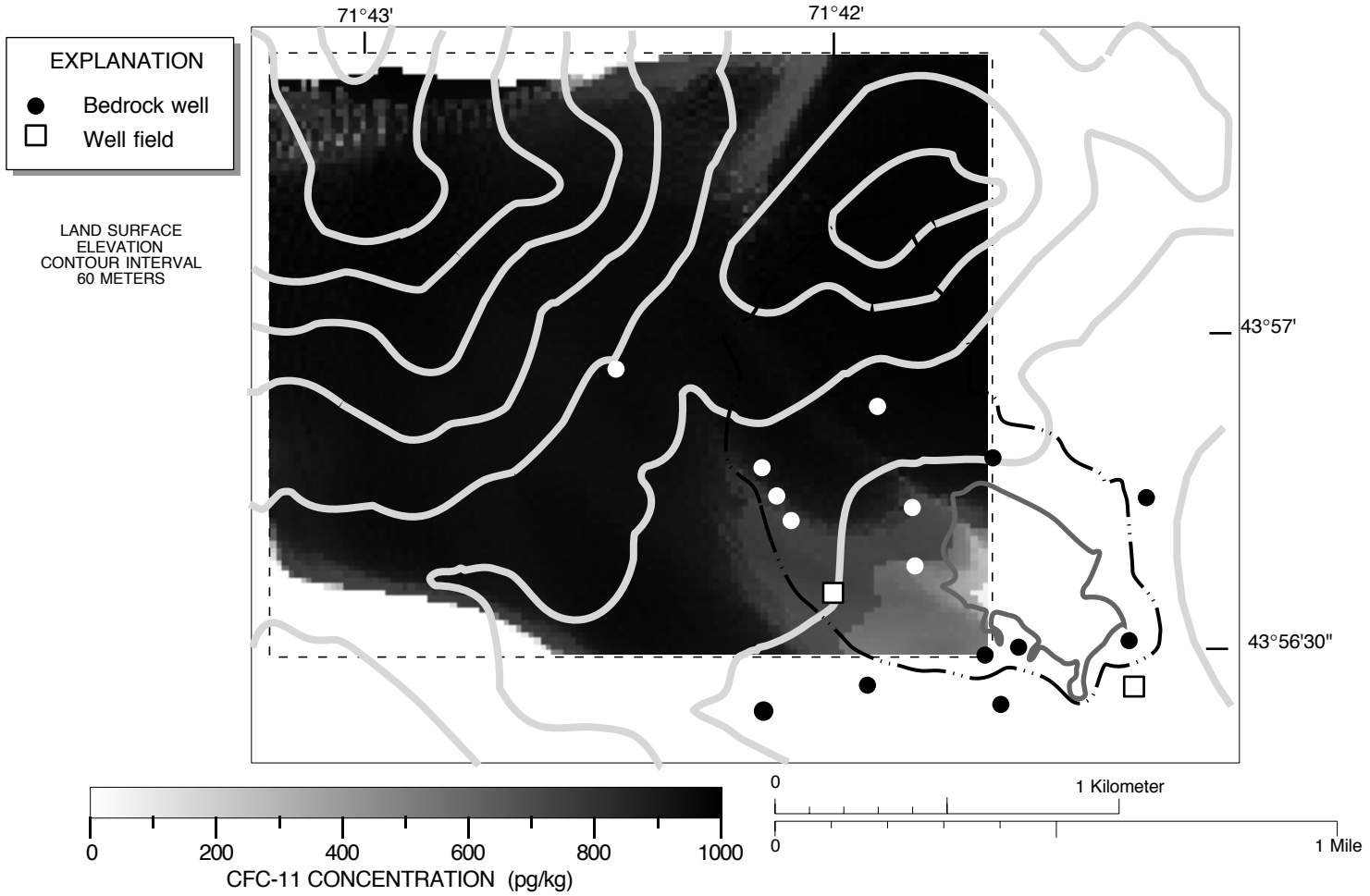

Figure 5-14 Simulated CFC-11 concentrations in deep bedrock from 90 meters below bedrock surface to 150 meters below the bedrock surface for advection only using bedrock effective porosity of 0.005.

The CFC-11 concentrations in ground water reflect the atmospheric source function (fig. 5-15). Near the water table, the ground-water concentration is essentially coincident with the atmospheric equilibrium level. A lag between the atmospheric level and the ground-water concentration occurs in deeper parts of the aquifer, depending on the advective travel times. For this case having low porosity, the lag between the water table and deeper concentrations is small, where the water table occurs in bedrock.

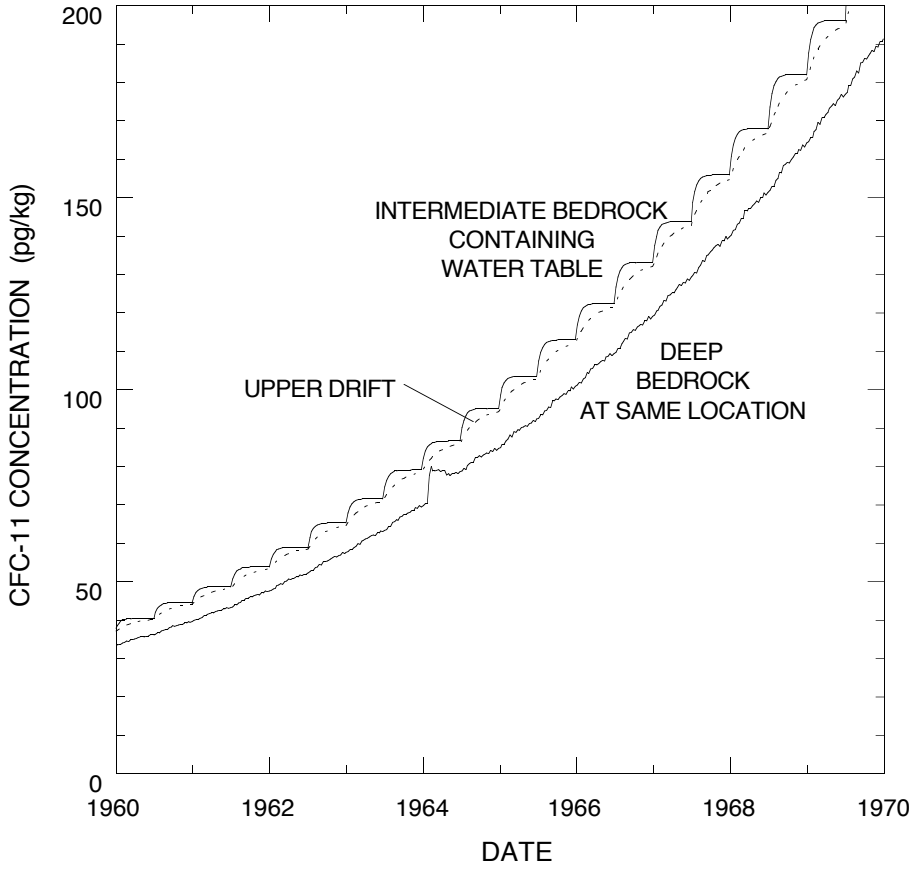

Figure 5-15 CFC-11 concentrations versus time in recharge areas for transport by advection only using bedrock effective porosity of 0.005.

The perturbation in the simulated concentrations for the deep bedrock are associated with particle regeneration in the method-of-characteristics numerical model

(Konikow et al., 1996). Particles are added to the domain as they leave fluid sources. When the maximum number of particles is reached, the initial uniform distribution of particles is regenerated, but with the current concentrations from the model nodes. As shown, this causes a temporary perturbation in computed concentrations that dissipates as particles redistribute themselves along flow lines. Konikow and Bredehoeft (1978) discuss fluctuations in computed concentrations associated with this discrete numerical method. Concentrations in the upper bedrock closely mirror the atmospheric levels when the water table is within the bedrock. The input source function has step changes in concentration every 6 months, and the bedrock water-table concentrations respond quickly to this step change because of the low storage in the rock.

5.5.2 Matrix Diffusion

The impact of matrix diffusion on CFC-11 concentrations depends on the relative porosity of the rock matrix and the fracture system, and the rate of diffusion in the rock matrix. Here, the simple double porosity model (Chapter Two) is used to approximate the effects of matrix diffusion. For these simulations, the bedrock effective porosity is 0.005, and the porosity of the immobile water zone in the rock matrix is 0.045. Hence, the total aquifer porosity is the same as the high-porosity case, 0.05. The limiting cases of exchange rate coefficient correspond to the advection-only cases. If the exchange coefficient is very high, then CFC-11 exchanges very quickly between the flowing fractures and the immobile zone. In this case, the effect is that the apparent solute velocity corresponds to the total porosity, 0.05, not just that of the fractures. At the other extreme, the rate of exchange between the rock matrix and the fractures is so slow that transport of CFC-11 is not significantly affected, and the aquifer's apparent effective porosity corresponds to that of the fractures alone, in this case 0.005. The exchange coefficient used here, 10^{-4} day^{-1}, yields transport results intermediate between these extremes (figs. 5-16 and 5-17).

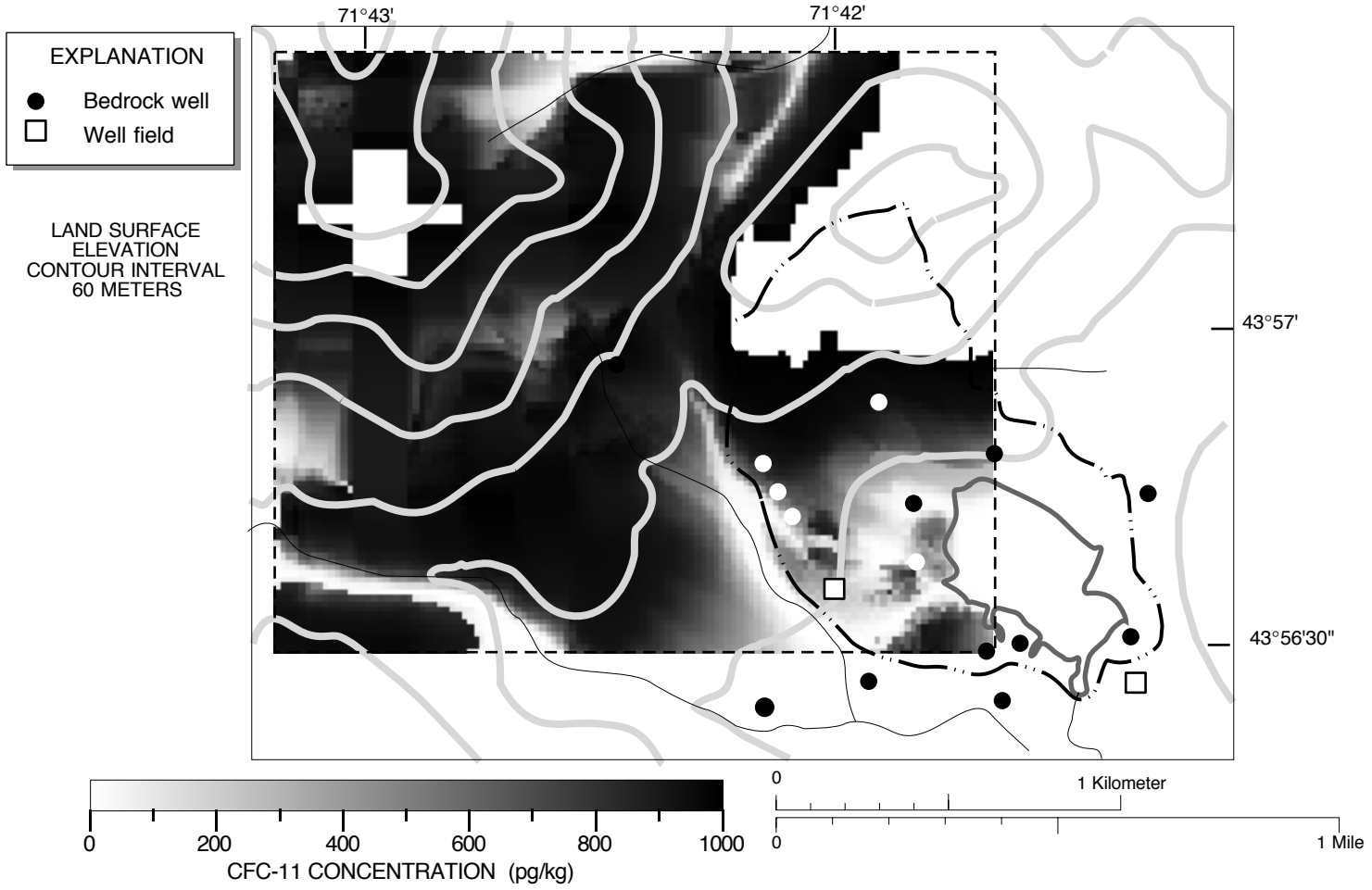

Figure 5-16 Simulated CFC-11 concentrations in upper bedrock from bedrock surface to 30 meters below bedrock surface for advection and matrix diffusion using bedrock effective porosity of 0.005, rock matrix porosity of 0.045 and exchange rate coefficient of 10^{-4} day^{-1}.

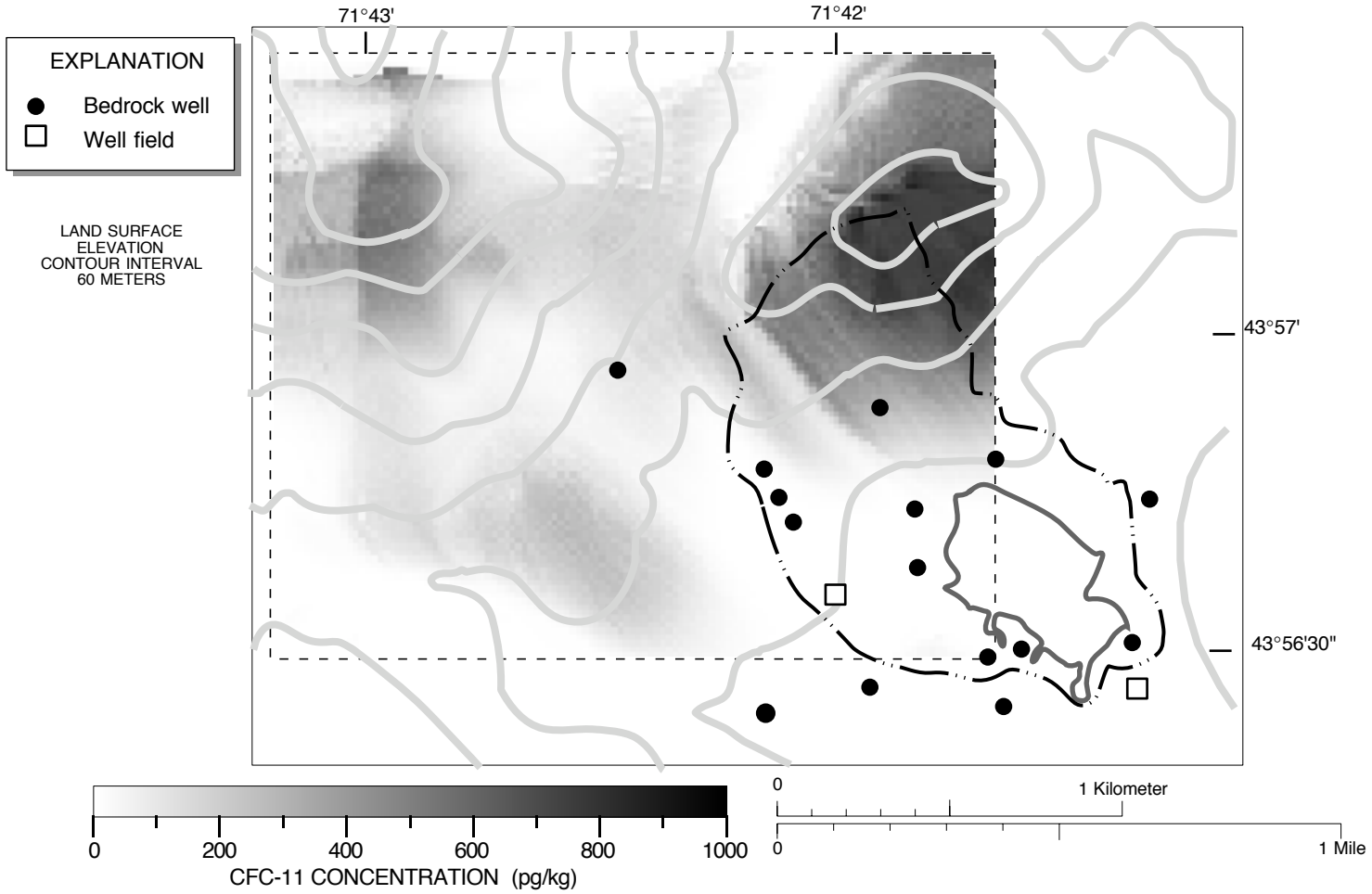

Figure 5-17 Simulated CFC-11 concentrations in deep bedrock from 90 meters below bedrock surface to 150 meters below bedrock surface for advection and matrix diffusion using bedrock effective porosity of 0.005, rock matrix porosity of 0.045 and exchange rate coefficient of 10^{-4} day^{-1}.

The effect of matrix diffusion is most apparent for the deep bedrock concentrations (fig. 5-17). Concentrations in deep bedrock are much lower than those for the case with the same effective porosity, but without matrix diffusion (fig. 5-14). This apparent increase in travel time is due to the retarding effect of rapid exchange between the flowing water in the fractures and the immobile water within the rock matrix. These results are more similar to the advective transport simulation with the high porosity value (fig. 5-12). One difference is that for the matrix diffusion case CFC-11 is present, albeit at low concentrations, throughout a larger part of the deep bedrock. This reflects the kinetics of the exchange process: most, but not all, of the CFC-11 is removed by diffusion into the rock matrix, but low concentrations persist in the flowing water zone because the exchange is not instantaneous.

The apparent increase in travel time through bedrock caused by matrix diffusion is also shown in the concentration histogram (fig. 5-18). Bedrock concentrations are lower and the lag between the water table in bedrock and underlying deep bedrock is substantially increased. The previously noted perturbation due to particle regeneration in the numerical method occurs at a little earlier in this simulation. Although the particle motion in the numerical model is identical for the cases with and without matrix diffusion, fewer particles were used in this case because of the additional computer storage required for the matrix-diffusion terms.

Matrix diffusion changes CFC-11 concentrations significantly only for certain values of the exchange-rate coefficient (β) (fig. 5-19). If β is greater than about 10^{-4} day^{-1}, then exchange is so rapid that concentrations in the fractures are essentially the same as if the effective porosity is equal to the total porosity. If β is less than about 10^{-6} day^{-1}, then matrix diffusion does not significantly impact CFC-11 concentrations during the time scale of this simulation. If the exchange-rate coefficient is within this range at the site, then this additional parameter will have to be incorporated in models to accurately estimate effective porosity from CFC-11 concentrations in bedrock.

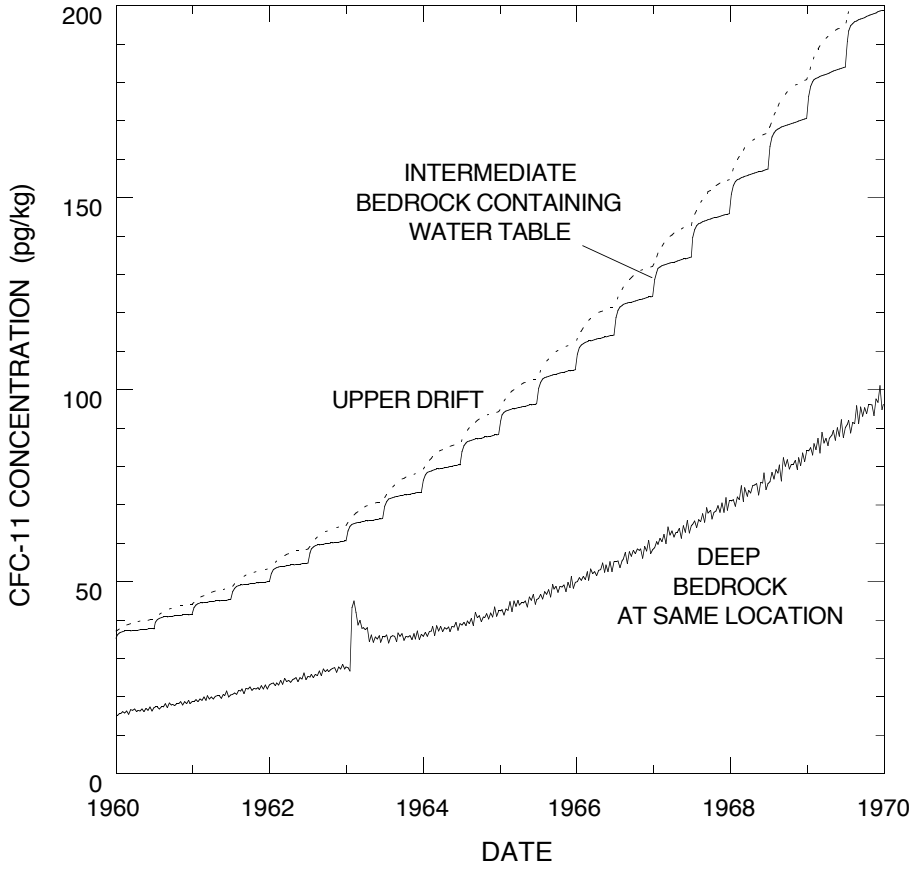

Figure 5-18 CFC-11 concentrations versus time in recharge areas for transport by advection and matrix diffusion using bedrock effective porosity of 0.005, rock matrix porosity of 0.045 and exchange rate coefficient of 10^{-4} day^{-1}.

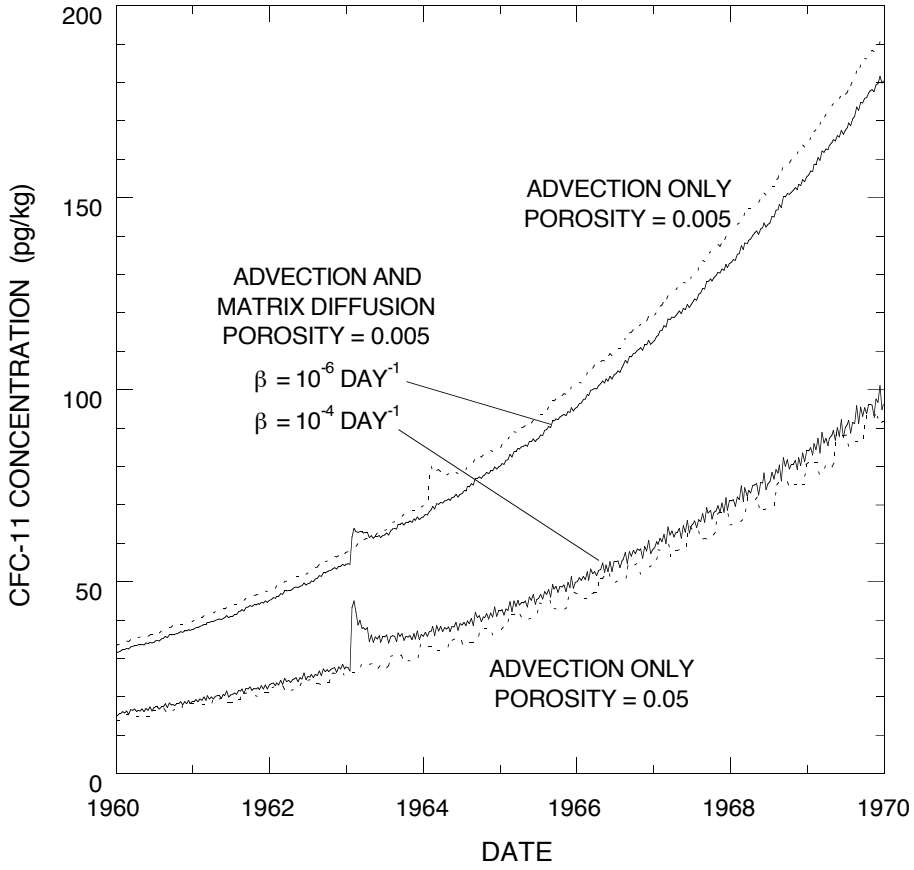

Figure 5-19 CFC-11 concentrations versus time for deep bedrock in recharge area for cases of transport by advection using bedrock effective porosities of 0.05 and 0.005, and transport by advection and matrix diffusion using bedrock effective porosity of 0.005, rock matrix porosity of 0.045 and exchange rate coefficients of 10^{-6} and 10^{-4} day^{-1}.

5.6 Summary

Preliminary simulations are conducted of age and CFC-11 transport in ground water at the Mirror Lake site, New Hampshire. The underlying connection between CFC concentrations and ground-water age is illustrated by the correspondence between simulated age and CFC-11 concentrations. CFC-depleted streamflow discharge to the glacial drift has a local impact on simulated CFC concentrations in the upper bedrock. Spatially variable age and CFC concentrations are simulated in the lower parts of the basin where local topographic highs occur next to discharge zones.

Steady-state age is insensitive to the diffusion rate for cases with matrix diffusion, but the CFC-11 concentrations are significantly different for different rates. Generally, the porosities required in the transport model to match age and CFC concentrations at the Mirror Lake site are higher than values measured on rock cores.

5.7 References

Busenberg, E., and Plummer, L.N., 1996, Concentrations of chlorofluorocarbons and other gases in ground water at Mirror Lake, New Hampshire: in Morganwalp, D.W., and Aronson, D.A., eds., U.S. Geological Survey Toxics Program Meeting, Colorado Springs, Colo., September 20-24, 1993: U.S. Geological Survey WRIR 94-4015.

Drenkard, S., Torgersen, T., Weppernig, R., Stute, M., Farley, K., and Schlosser, P., 1993, Helium isotopes and tritium-helium age dating: Mirror Lake, New Hampshire (abs.): GSA Abstracts with Programs, v. 25, no. 6, p. A-364.

Harte, P.T., 1992, Regional ground-water flow in crystalline bedrock and interaction with glacial drift in the New England uplands: M. S. Thesis, University of New Hampshire, Durham, 147 p.

Harte, P.T. and Winter, T.C., 1995, Simulations of flow in fractured crystalline rock in a hypothetical New England setting: Ground Water, v. 33, no. 3, p. 953-964.

Hill, M.C., 1992, A computer program (MODFLOWP) for estimating parameters of a transient, three-dimensional, ground-water flow model using nonlinear regression: U.S. Geological Survey Open-File Report 91-484, 358 p.

Hsieh, P. A., Shapiro, A. M., Barton, C. C., Haeni, F. P., Johnson, C. D., Martin, C. W., Paillet, F. L., Winter, T. C., and Wright, D. L., 1993, Methods of characterizing fluid movement and chemical transport in fractured rock: in Chaney, J. T., and Hepburn, C., (eds.) Field Trip Guidebook for northeastern United States, Geological Society of America, annual Meeting, October 25-28, 1993, Boston, Mass., v. 2, chap. R, p. R1-R23.

Konikow, L.F., D.J. Goode and G.Z. Hornberger, A three-dimensional method-of-characteristics solute-transport model (MOC3D): U.S. Geological Survey Water-Resources Investigations Report 96-4267, 87 p.

McDonald, M.G., and Harbaugh, A.W., 1988, A modular three-dimensional finite-difference ground-water flow model: U.S. Geological Survey Techniques of Water-Resources Investigations, book 6, chap. A1, 586 p.

Plummer, L. N., R.L. Michel, E.M. Thurman, and P.D. Glynn, 1993,. Environmental tracers for age dating young ground water, in *Regional Ground-Water Quality* , edited by W. M. Alley, pp. 255-294, Van Nostrand Reinhold, New York.

Rosenberry, D.O., and Winter, T.C., 1993, The significance of fracture flow to the water balance of a lake situated in fractured crystalline rock terrain, in Banks, Sheila, and Banks, David, eds., IAH Memoires of the 24th Congress, Hydrogeology of Hard Rock, As, Norway, June 28 to July 2, 1993: International Association of Hydrogeologists, p. 967-977.

Shapiro, A.M., 1996, Using environmental tracers to estimate matrix diffusion in fractured rock over distances of kilometers: Results from the Mirror Lake site, New Hampshire: Eos, Trans. AGU, v. 77, no. 17, p. S107.

Shapiro, A. M., and P. A. Hsieh, 1991, Research in fractured-rock hydrogeology: Characterizing fluid movement and chemical transport in fractured rock at the Mirror Lake drainage basin, New Hampshire: p. 155-161 in Mallard, G.E., and D. A. Aronson (eds.), U.S. Geol. Survey Toxic Substances Hydrology Program--Proc. Technical Meeting, Monterey, California, March 11-15, 1991: U.S. Geol. Survey Water-Resources Invest. Rep. 91-4034.

Shapiro, A.M., Wood, W.W., Busenberg, E., Drenkard, S., Plummer, L.N., Torgersen, T., and Schlosser, P., 1996, Conceptual model for estimating regional fluid velocity in the bedrock of the Mirror Lake area, Grafton County, New Hampshire, *in* Toxics Program Meeting, Colorado Springs, U.S. Geological Survey WRIR 94-4015.

Tiedeman, C.R., Goode, D.J., and Hsieh, P.A., 1997, Numerical simulation of ground-water flow through glacial deposits and crystalline bedrock in the Mirror Lake area, Grafton County, New Hampshire: U.S. Geological Survey Professional Paper 1572, 50 p.

Winter, T. C., 1984, Geohydrologic setting of Mirror Lake, West Thornton, New Hampshire: U.S. Geological Survey Water-Resources Investigations Report 84-4266, 61 p.

Winter, T. C., 1985, Physiographic setting and geologic origin of Mirror Lake: in Likens, G. E., ed., *An ecosystem approach to aquatic ecology: Mirror Lake and it Environment*: Springer-Verlag, New York, p. 40-53.

Winter, T. C., Eaton, J. S., and Likens, G. E., 1989, Evaluation of inflow to Mirror Lake, New Hampshire: Water Resources Bulletin, vol. 25, no. 5, p. 991-1008.

Wood, W.W., Shapiro, A.M., and Councell, Terry, 1996, Observational experimental and inferred evidence for solute diffusion in fractured granite aquifers: Examples from Mirror Lake Watershed, Grafton County, New Hampshire: in Morganwalp, D.W., and Aronson, D.A., eds., U.S. Geological Survey Toxics Program Meeting, Colorado Springs, Colo., September 20-24, 1993: U.S. Geological Survey WRIR 94-4015.